Ion−Molecule Reaction Studies of Hydroxyl Cation and Ionized Water with Ethylene

Vyacheslav N. Fishman and Joseph J. Grabowski*

Department of Chemistry, University of Pittsburgh, Pittsburgh, Pennsylvania 15260

Received: January 19, 1999; In Final Form: April 28, 1999

Rate coefficients and product branching ratios for the ion−molecule reactions of the hydroxyl cation, ionized water, and their deuterated analogues with ethylene have been determined using a selected ion flow tube (SIFT) at room temperature and in 0.5 Torr of helium buffer gas. In all cases, reactions proceed at or near the collision rate. The major product is always charge transfer: 79% for $L_2O^{\bullet+}$ and 66% for LO^+ and does not depend on the isotopic form of hydrogen present (L = H or D). For the $L_2O^{\bullet+}$ reactions, the remaining 21% of products are from proton or deuteron transfer, with no evidence of an isotope effect on this step even in the $HOD^{\bullet+}$ reaction. The greater exothermicity of the initial charge transfer in the LO^+ reaction is revealed by the observation of additional product channels, forming the vinyl cation and protonated carbon monoxide. Multistep mechanisms that proceed through rate-determining charge-transfer, followed by a product-determining step, are postulated to explain these observations.

Introduction

Detailed information about gas-phase ion−molecule reactions can lead to a better understanding of the chemical composition of interstellar gas clouds,[1,2] planetary atmospheres,[3] combustion processes,[4−6] and even chemical ionization mass spectrometry.[7] The ions HO^+ and $H_2O^{\bullet+}$, and their deuterated analogues, are extremely reactive species that contribute to each of these chemical environments. Ethylene is a known component of circumstellar shells[1,2] and is produced by photochemical and thermal reactions involving methane in the hydrogen-rich envelope on the Jovian planets[3] (Jupiter, Saturn, Uranus, and Neptune). The contribution of ethylene in combustion processes of hydrocarbon fuels such as gasoline and kerosene has long been known.[4]

Isotopic fractionation of H-to-D in various molecules is important when interpreting cosmic origins and abundances. Some molecules are known to show an enhanced D-to-H ratio that exceeds the conventional ratio by an order of magnitude or more.[8,9] Previous tandem mass spectrometry studies of several ion−molecule reactions support the hypothesis that ion chemistry is important in understanding nonconventional ratios.[1,2] Isotopic labeling, of course, is also an important tool for gaining insight into a large variety of chemical reactions.[10]

The reaction of $H_2O^{\bullet+}$ with C_2H_4 has been examined previously; Dotan et al.,[11] using a flow-drift tube, were able to measure the rate coefficient as a function of kinetic energy (0.03−2 eV) in helium with $k_{300\ K} = 16\ (\pm 4.8) \times 10^{-10}$ cm^3 molecule^{-1} s^{-1}, but were unable to determine the reaction products. Rakshit and Warneck,[12] using a drift chamber mass spectrometer, examined $H_2O^{\bullet+}$ with C_2H_4 in CO_2 and reported a rate coefficient (at undefined interaction energy and accuracy) of 1.5×10^{-9} cm^3 molecule^{-1} s^{-1}, and stated that the reaction proceeds exclusively by charge transfer. Ion−molecule studies of extremely reactive species such as an $H_2O^{\bullet+}$ and HO^+ can be challenging; Shul et al.[13] were able to investigate several such systems only by simultaneously injecting HO^+, $H_2O^{\bullet+}$, and H_3O^+ and at the cost of both being able to determine reliable branching ratios and increased error limits on rate coefficients. Here, we demonstrate how our recently described SIFT injector flange[14] is capable of allowing high-quality quantitative data to be collected for both rate coefficients and branching ratios, by characterizing the reactions of $L_2O^{\bullet+}$ and LO^+, where L = H or D, with $H_2C{=}CH_2$.

Experimental Section

All of the measurements reported here were performed with the University of Pittsburgh's selected ion flow tube (SIFT), the details of which have been previously described;[14] only those experimental details unique to this study are reported here. Reactant ions were produced in a Brinks type ionizer[15] using electron ionization on water vapor: H_2O for HO^+ and $H_2O^{\bullet+}$; D_2O for DO^+ and $D_2O^{\bullet+}$; and the vapor from a 3:1 liquid-phase mixture of D_2O:H_2O for production of $HOD^{\bullet+}$. The potential difference between the filament and grid was selected (20−30 eV) to minimize production of excited states in the reactant ion. At the same time, the potential of the grid with respect to the grounded reaction tube was kept as low as possible both to minimize the kinetic energy of the ions produced (in order to improve ion separation in the first quadrupole) and to decrease the likelihood of collision-induced dissociation (CID) during the injection process. All ion−molecule measurements were carried out in the presence of helium buffer gas at a pressure of 0.46−0.53 Torr and a temperature of 298 (±1) K. High-purity helium (99.997%) was further purified by passage through a liquid nitrogen cooled molecular-sieve trap before use.[14] Ethylene (technical grade, 98%) was used as received. The error bars reported are one standard deviation based upon repeated measurements taken over at least two experimental days. We estimate the absolute error limits on a reported rate coefficient, k_{obs}, to be 20%, due to systematic errors involved in measurements of neutral and buffer gas flows and pressures.[16,17] Reaction efficiency, Eff, is the ratio k_{obs}/k_{coll} and is based on a collision rate coefficient, k_{coll}, calculated according to the variational collision complex theory developed by Su and Chesnavich.[18] The absolute error limit on the primary product yields is estimated to be no more than 5%. For the very fast reactions being examined in this study, with equally fast secondary

10.1021/jp990226s CCC: $18.00
Published on Web 06/06/1999

reactions, trace ion products (≤2% of the total products) are difficult to quantify and therefore are omitted from consideration.

Results

Due to the high reactivity of the ions under study with water, and the difficulty of eliminating all adventitious water from the helium,[16] we tested our instrument for its ability to cleanly inject $D_2O^{\bullet+}$ by first creating, selecting, and injecting *m*/*z* 20 in the absence of the He buffer gas.[16] The spectra shown in Figure 1a and b demonstrate that clean injection of only *m*/*z* 20 can be achieved in our instrument. After just a single *m*/*z* value is selected and injected into the He-filled reaction tube, it may react with the 0.4 ppm of H_2O^{16} still present in the purified helium. Thus when we inject $D_2O^{\bullet+}$ into the He-filled reaction tube, we typically see spectra similar to Figure 1c. The reaction of $D_2O^{\bullet+}$ (*m*/*z* 20) with H_2O has been studied by Anicich and Sen in an ICR;[19] they found a rapid reaction ($k_{obs} = 1.56$ (+0.78, −0.22) × 10^{-9} cm^3 molecule^{-1} s^{-1}; Eff = 54%) gives 21% *m*/*z* 18, 19% *m*/*z* 19, and 59% *m*/*z* 21. In our experiment, (e.g., Figure 1c) we attribute the *m*/*z* 21, *m*/*z* 19, and a portion of the *m*/*z* 18 signal to the reaction of $D_2O^{\bullet+}$ with adventitious water. The *m*/*z* 18 peak also reflects a small amount of a CID process (eq 1) that we are unable to completely eliminate while retaining adequate signal.

$$D_2O^{\bullet+} \xrightarrow[\text{CID}]{\text{He}} DO^+ + D^\bullet + \Delta H_{rxn} = 130.3 \text{ kcal mol}^{-1} \quad (1)$$

The presence of the small amounts of these other ions contributes to the larger than normal error bar on the branching ratios reported. However, their contribution is minimal due to their trace nature and the added fact that upon addition of ethylene the $H_2O^{\bullet+}$ will preferentially react with the much more abundant ethylene (~35 ppm).

The bimolecular rate coefficients obtained in the present study are summarized in Table 1. The error bars for k_{obs} indicate the precision of our experimental data, one standard deviation.

The most challenging aspect of characterizing many ion−molecule reactions is a determination of its branching ratio, the relative yield of the competitive product channels. The branching ratios summarized in Table 1 are the average of 3−6 independent measurements, each of which consists of data collected by varying either the reaction distance at fixed ethylene concentration or by varying ethylene concentration at fixed reaction distance (time).[16] In all cases the reactions were followed to between 30 and 60% completion in order to minimize complications from facile secondary reactions.[20,21] An example of one typical experimental measurement of the branching ratio for the reaction of $H_2O^{\bullet+}$ with ethylene is shown in Figure 2. All branching ratios reported in the Table 1 represent a compilation of data from similar plots.

$L_2O^{\bullet+}$ + $H_2C{=}CH_2$. Formal charge (CT) and proton transfer (PT) leads to the observed *m*/*z* 28 and 29 product ions with the relative ratio of 78:22 for the reaction of $H_2O^{\bullet+}$ with $H_2C{=}CH_2$. The reaction of $D_2O^{\bullet+}$ with $H_2C{=}CH_2$ similarly shows *m*/*z* 28 (CT) and 30 (deuteron transfer, DT) as 83:17 (see Figure 1d), while the reaction of $HOD^{\bullet+}$ with $H_2C{=}CH_2$ gives *m*/*z* 28 (CT), 29 (PT), and 30 (DT) as 77:12:11. The efficiency for $H_2O^{\bullet+}$ + $H_2C{=}CH_2$ reported as 106% in Table 1 might be misleading; the larger than 100% value likely reflects errors in k_{obs} and error in the assumptions used to derive k_{coll}.[18]

LO^+ + $H_2C{=}CH_2$. The reactions of HO^+ and DO^+ with $H_2C{=}CH_2$ are essentially identical and show CT as the major channel (66%). Both reactions also yield 12% of *m*/*z* 27, the vinyl cation, formed via hydride transfer. The remaining 22% of the products appear to be from PT in the HO^+ reaction but, as revealed by the DO^+ reaction, actually result from a combination of proton transfer (15%) and fragmentation to yield LCO^+ (7%). For these LO^+ reactions, any trace primary product ions (≤2% of the total ion product yield) at *m*/*z* 30, 31, and/or 32 are difficult to reproducibly quantify due to their low abundance and fast secondary reactions and therefore are omitted

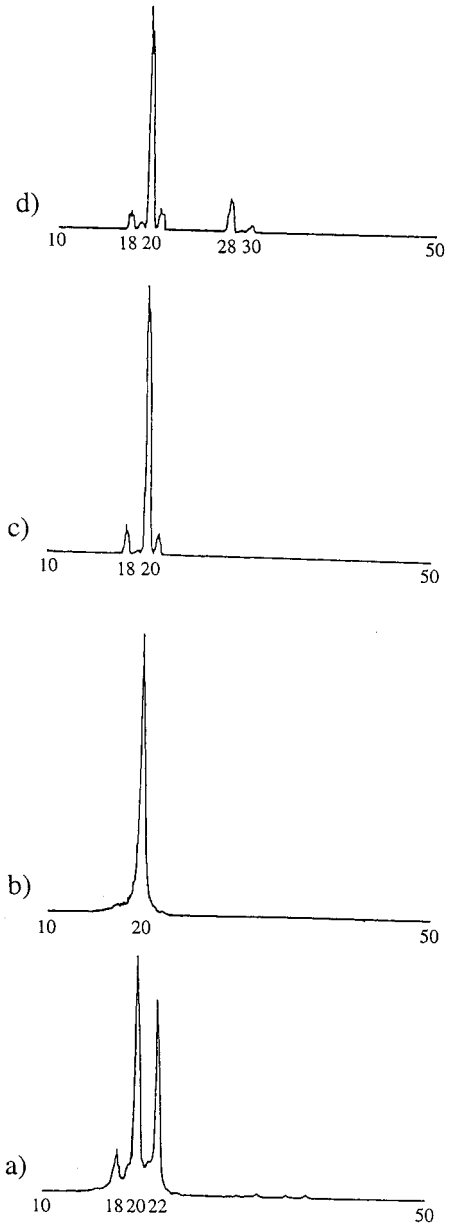

Figure 1. Mass spectra demonstrating the injection capability of the SIFT for $D_2O^{\bullet+}$ and its subsequent reaction with ethylene. (a) The mass spectrum of ions produced in the ion source region as observed via the detection system when the selection quadrupole is operated in total transmission mode and there is no buffer gas in the 150 cm long flow tube. (b) A mass spectrum obtained under the same conditions as in (a) wherein the only difference is that the selection quadrupole transmits only *m*/*z* 20, $D_2O^{\bullet+}$. (c) An example of a typical "reactant ion spectrum" for the $D_2O^{\bullet+}$ studies with the transmission quadrupole selecting *m*/*z* 20 and the flow tube is filled with 0.5 Torr of He. As described in the text, the *m*/*z* 18, 19, and 21 ions result principally from reaction of $D_2O^{\bullet+}$ with adventitious water and partially from CID of $D_2O^{\bullet+}$. (d) An example of a mass spectra obtained during the early portion of the reaction of $D_2O^{\bullet+}$ with $H_2C{=}CH_2$; *m*/*z* 28 is $C_2H_4^{\bullet+}$ and *m*/*z* 30 is $C_2H_4D^+$. All spectra shown here are single scans (no averaging) obtained at a scan rate of 0.5 amu s^{-1}.

TABLE 1: Summary of Kinetic Data for the Reaction of $L_xO^{\bullet+}$ ($x = 1, 2$) with Ethylene in 0.5 Torr of Helium at 298 K

	IP[a] (eV)	k_{obs}[b] (cm^3 $molecule^{-1}$ s^{-1})	efficiency (%)	# $t_{1/2}$[c]	yield	m/z[c]	ion product[d]	ΔH_{rxn}[a] (kcal/mole)
$H_2O^{\bullet+}$	12.62	15.5 ($\pm$0.4) $\times$ 10^{-10}	106%[e]	6.2	78%	28	$C_2H_4^{\bullet+}$	−48.7
					22%	29	$C_2H_5^+$	−20.9
$HOD^{\bullet+}$	12.63	11.0 ($\pm$0.2) $\times$ 10^{-10}	77%	1.5	77%	28	$C_2H_4^{\bullet+}$	−48.9
					12%	29	$C_2H_5^+$	−20.8
					11%	30	$C_2H_4D^+$	−17.7
$D_2O^{\bullet+}$	12.64	9.48 ($\pm$0.5) $\times$ 10^{-10}	67%	6.8	83%	28	$C_2H_4^{\bullet+}$	−49.1
					17%	30	$C_2H_4D^+$	−17.6
HO^+	13.02	14.8 ($\pm$0.9) $\times$ 10^{-10}	99%	5.5	13%	27	$C_2H_3^+$	−123.3
					66%	28	$C_2H_4^{\bullet+}$	−63.1
					21%	29	$C_2H_5^+$	−52.2
							and/or $HC{\equiv}O^+$	−41.0
DO^+	13.03	15.9 ($\pm$1.2) $\times$ 10^{-10}	109%[e]	3.3	11%	27	$C_2H_3^+$	−118.6
					67%	28	$C_2H_4^{\bullet+}$	−58.1
					7%	29	$HC{\equiv}O^+$	−34.6
					15%	30	$C_2H_4D^+$	−44.1

[a] *NIST Chemistry WebBook, NIST Standard Reference Database Number 69*; Mallard, W. G., Linstrom, P. J., Eds.; National Institute of Standards and Technology (http://webbook.nist.gov): Gaithersburg, MD; March 1998. [b] The error reported is one standard deviation of the average. See text for a discussion of the kinetic models used to extract these bimolecular rate coefficients from the observed data. [c] The average number of half-lives used to determine the rate coefficient. [d] Only reaction products that are ≥2% of the overall yield are reported. [e] See text for a discussion of Eff > 100%.

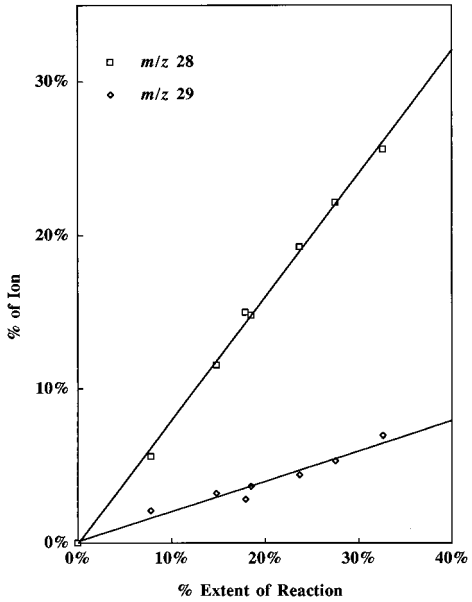

Figure 2. An example of one branching ratio experiment for the reaction of $H_2O^{\bullet+}$ with $H_2C{=}CH_2$ in 0.5 Torr of He at 298 K. The fit of the observed points to a straight line demonstrates that secondary reactions are not yet contributing to the observed ion yields. The slopes of the lines for this one experiment give the product yield of 80% of m/z 28 and 20% of m/z 29.

from consideration. As for the $H_2O^{\bullet+}$ reaction, the 109% efficiency in Table 1 for the DO^+ reaction reflects errors in k_{obs} and/or k_{coll}.

Discussion

The rate coefficient reported here, 1.55 ($\pm$0.04) $\times$ 10^{-9} cm^3 $molecule^{-1}$ s^{-1}, for the reaction of $H_2O^{\bullet+}$ with $H_2C{=}CH_2$, is in excellent agreement with that reported by Dotan et al.[11] as 1.6 ($\pm$0.5) $\times$ 10^{-9} cm^3 $molecule^{-1}$ s^{-1}, at 300 K, as determined in a flow-drift tube, as well as that reported by Rakshit and Warneck[12] as 1.5 $\times$ 10^{-9} cm^3 $molecule^{-1}$ s^{-1} as determined in a drift chamber mass spectrometer. The unit efficiency clearly indicates that the rate-determining step for the reaction is the collision rate. In addition, we are able to identify the products as 78% from a formal CT process and 22% from a formal PT process. We next examined $D_2O^{\bullet+}$ with $H_2C{=}CH_2$ and observed a significant drop in the reaction efficiency, to 67%, but an experimentally indistinguishable product yield of 83% formal CT and 17% formal DT. The data for $D_2O^{\bullet+}$ (as compared to that for $H_2O^{\bullet+}$) suggest that the collision is no longer the sole rate-determining step, and that the rate-determining step for both reactions is not the same as the product-determining step.

The branching ratio we determined for $H_2O^{\bullet+}$ with $H_2C{=}CH_2$ is somewhat different than that determined by Rakshit and Warneck who observed only the CT channel. We are unsure of the reasons for the difference but two possibilities suggest themselves. The first is that the interaction energy in their experiment is suprathermal; for a multistep chemical transformation (as we suggest below) this would favor products earlier in the reaction sequence (i.e., would enhance CT over PT, vide infra).[22] The second possibility is that the complicated reaction sequence and fitting procedure employed in their study was unable to accurately identify all the products.

To gain additional information, we next examined the reaction of $HOD^{\bullet+}$ with $H_2C{=}CH_2$. This presents a challenge as there are two reactive isobaric ions at m/z 19, $HOD^{\bullet+}$ and H_3O^+, and no convenient way to exclusively prepare and study just $HOD^{\bullet+}$. The reaction of H_3O^+ with $H_2C{=}CH_2$ has been studied before in helium[23,24] carrier gas; the study by Matthews et al.[24] in 0.50 Torr of helium indicates that reaction proceeds according to eq 2.

$$H_3O^+ + H_2C{=}CH_2 \xrightarrow[0.5\ \text{Torr He}]{k_{obs} = 7.8 \times 10^{-11}} 65\%\ C_2H_5^+ + H_2O \quad (2a)$$

$$35\%\ C_2H_7O^+ \quad (2b)$$

To ensure the major reactant ion injected at m/z 19 in our experiment is $HOD^{\bullet+}$, we electron ionized a 3:1 (liquid phase) mixture of D_2O: H_2O. This should ensure a low relative abundance of H_3O^+ but will not completely eliminate its contribution in the injected signal. Because of the relatively slow reaction of H_3O^+ compared to $D_2O^{\bullet+}$, $H_2O^{\bullet+}$, and (presumably) $HOD^{\bullet+}$, as well as the fact that the branching ratio measurements are determined from the first 40% of reaction or less (for this reaction), we are able to determine the yields reported in Table 1 in good confidence. This confidence in the branching ratio data is reinforced by the lack of observation of $C_2H_7O^+$ under

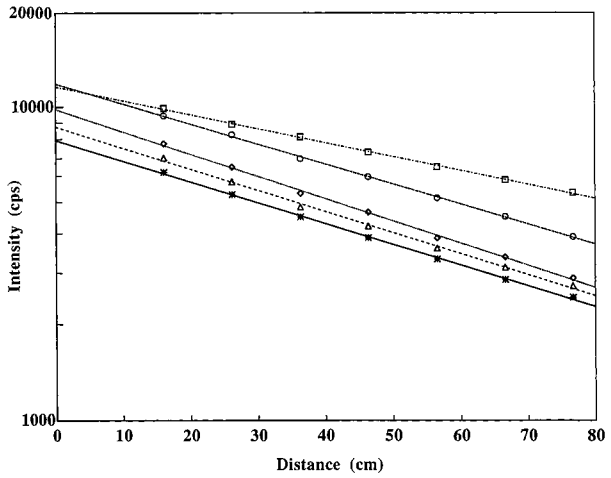

Figure 3. Experimental data for the observed decay of *m*/*z* 19 (points) for the reaction of $HOD^{\bullet+}$ with $H_2C{=}CH_2$ for five different experiments. In each case, the straight line is a fit to a standard pseudo-first-order kinetic model that assumes only one reactant is present at *m*/*z* 19. The intensity data represents average counts per second determined for a total counting time of 5 s.

the conditions used. As shown in Table 1, the reaction of $HOD^{\bullet+}$ with $H_2C{=}CH_2$ yields the same product distribution as the previous two reactions, 77% CT, and 23% proton/deuteron transfer. The identical product yield with the previous reactions, along with equivalent yields of proton and deuteron transfer, are consistent with the absence of any isotope effect in the product-determining step.

The kinetic characterization of the $HOD^{\bullet+}$ with $H_2C{=}CH_2$ reaction is more problematic; normally our kinetic measurements in the SIFT follow reactions for ~5 or more half-lives. However, the presence of two reactive, isobaric ions at *m*/*z* 19, in unknown concentrations, precludes our standard measurement since all pseudo-first-order kinetics plots followed over 5 or more half-lives are severely curved, indicating two distinct reacting species. We therefore obtained an estimate for the rate coefficient for the $HOD^{\bullet+} + H_2C{=}CH_2$ reaction by using data for only the first ~50% decay of the initial $HOD^{\bullet+}$ signal (the average number of half-lives used is 0.9 averaged over 8 individual experiments) and a standard pseudo-first-order kinetic model. This analysis rigorously provides a lower limit to k_{obs} of 9.0×10^{-10} cm^3 $molecule^{-1}$ s^{-1} and visually looks to adequately fit the observations (Figure 3). However, a k_{obs} for $HOD^{\bullet+} + H_2C{=}CH_2$ of 9.0×10^{-10} corresponds to a reaction efficiency of only 63%, which is significantly less than that observed for the comparable $H_2O^{\bullet+}$ reaction.

A more correct treatment of the data would recognize that the observed decay of *m*/*z* 19 is due to the sum of the two kinetic processes, a fast reaction due to $DOH^{\bullet+} + H_2C{=}CH_2$ and a slower reaction due to $H_3O^+ + H_2C{=}CH_2$ (eq 2). If one assumes that the $DOH^{\bullet+}$ reaction occurs at the collision limit (i.e., identical to what is observed for the $H_2O^{\bullet+}$ reaction) and the H_3O^+ reaction occurs with the rate coefficient reported by Matthews et al.,[24] then the only variable needed to fit the observed kinetic data to the model is the relative concentration of H_3O^+ in the *m*/*z* 19 signal. One of our data sets, analyzed in exactly this fashion, is shown in Figure 4a. Note that in this figure, the only variable is the fraction of the *m*/*z* 19 signal that is H_3O^+ and this fraction was varied in order to obtain the best fit (shown by the solid line). As is clearly discernible in Figure 4a, the model poorly reproduces the experimental data leading to the conclusion that the $DOH^{\bullet+}$ reaction is not proceeding at the collision limit.

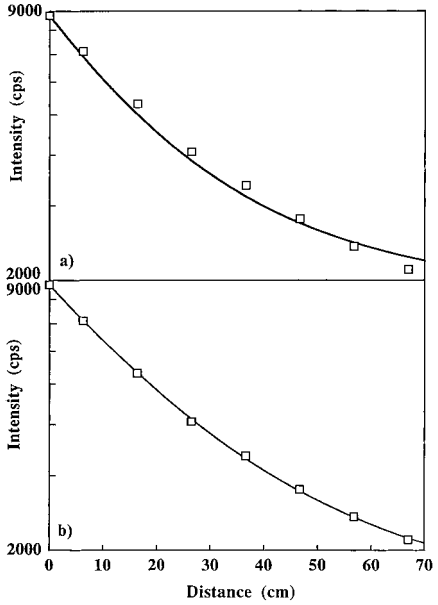

Figure 4. Representative experimental data (points) and fits to various models for the determination of the bimolecular rate coefficient for the reaction of $HOD^{\bullet+}$ with $H_2C{=}CH_2$ using a two-component kinetic model. The line represents a fit to a specific kinetic model. (a) Assumes the rate coefficient for $HOD^{\bullet+}$ is the collision rate coefficient and the rate coefficient for the H_3O^+ reaction as measured by Matthews et al. (ref 24); the only adjustable parameter is the relative concentration of H_3O^+ in the *m*/*z* 19 signal. (b) Like (a) but allows the rate coefficient of the $HOD^{\bullet+}$ reaction to vary as well.

We therefore reanalyzed the kinetic data for the $HOD^{\bullet+} + H_2C{=}CH_2$ reaction using a two-component kinetic model that allowed two reactive isobaric ions to be present: fraction *f* of which is $HOD^{\bullet+}$ reacting with an unknown rate coefficient and fraction $(1 - f)$ of which is H_3O^+ reacting with $k = 7.8 \times 10^{-11}$ cm^3 $molecule^{-1}$ s^{-1} (0.5 Torr He).[24] Figure 4b displays the results of the best fit of this model to the same data as presented in Figure 4a. This model clearly reproduces the experimental observations much better. In addition, this more correct model allows us to extend the useful range of the kinetic data beyond the first 50% decay. Nine separate kinetic runs, collected over two different experimental days, are all well fit by this two component model and return k_{obs} for the $HOD^{\bullet+}$ reaction of 1.1 ($\pm$0.1) $\times$ 10^{-9} cm^3 $molecule^{-1}$ s^{-1}. For these nine experiments, the average number of half-lives over which data was collected was 1.5, and was held low in order to maximize our sensitivity to the reaction we care about (the faster component). The relative concentration of H_3O^+ in the *m*/*z* 19 signal varied from a low of 9% to a high of 44%, and averaged 20%. We therefore conclude that the best rate coefficient to describe the reaction of $HOD^{\bullet+}$ with $H_2C{=}CH_2$ is 1.1×10^{-9} cm^3 $molecule^{-1}$ s^{-1} which corresponds to a reaction efficiency of 77%.

The reaction of $D_2O^{\bullet+}$ with $H_2C{=}CH_2$ potentially has a kinetic complication similar to that found in the $HOD^{\bullet+}$ reaction as *m*/*z* 20 could also be H_2OD^+. However, in the $D_2O^{\bullet+}$ reaction, the neutral precursor added to the ion source is pure D_2O, thus H_2OD^+ should present a much smaller problem than the corresponding complication in the $HOD^{\bullet+}$ study. Nonetheless, we treated the kinetic data for the $D_2O^{\bullet+}$ reaction using the same two-component model as for the $HOD^{\bullet+}$ reaction (we kept the rate coefficient for the H_2OD^+ fixed at the same value as for the H_3O^+ reaction). Data sets (8) collected over two different experimental days were fit and returned k_{obs} for $D_2O^{\bullet+} + H_2C{=}$

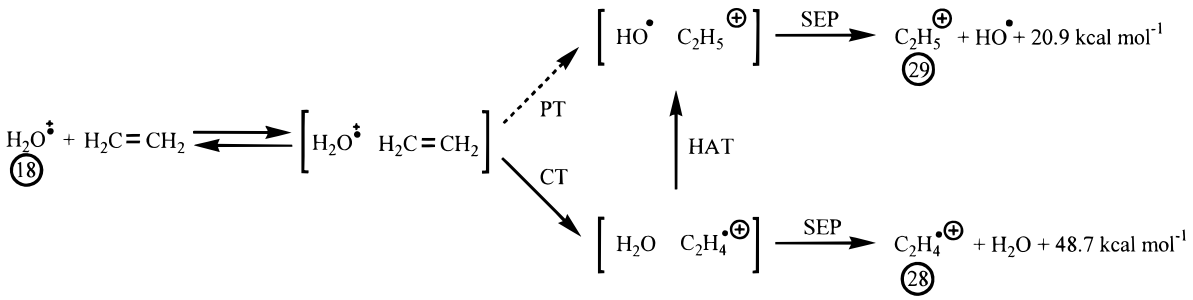

Figure 5. Mechanistic hypothesis for the reaction of $H_2O^{\bullet+}$ with ethylene at 300 K. Exothermic reaction channels are indicated by a positive energy yield.

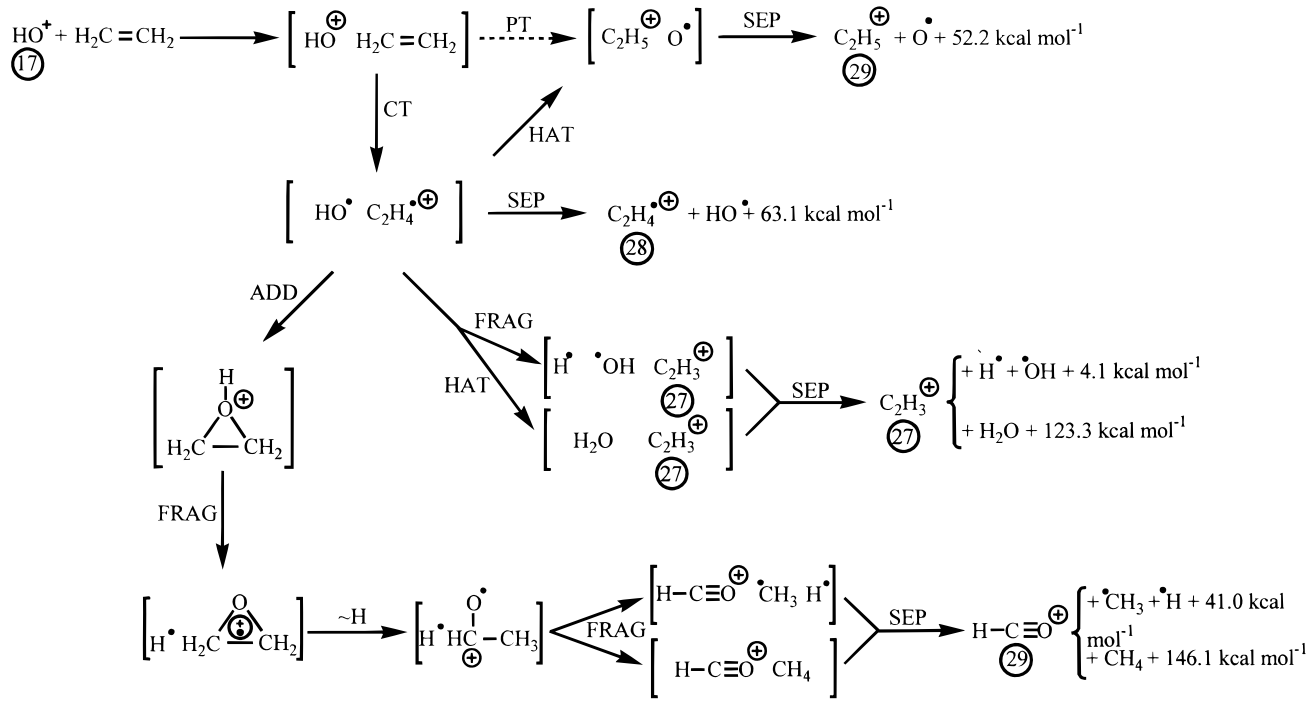

Figure 6. Mechanistic hypothesis for the reaction of OH^+ with ethylene at 300 K. Exothermic reaction channels are indicated by a positive energy yield.

CH_2 as 9.45 (±0.51) × 10^{-10} cm^3 $molecule^{-1}$ s^{-1} which corresponds to a reaction efficiency of 67%.

To summarize the $L_2O^{\bullet+} + H_2C{=}CH_2$ reaction data: all three isotopic variants react to give 79 (±5)% charge transfer and 21 (±5)% proton transfer with no distinction between proton or deuteron transfer in the case of $HOD^{\bullet+}$. Furthermore, there is a small, but reproducible reduction in reaction efficiency upon deuterium incorporation into the reactant ion; the $L_2O^{\bullet+}$ reaction proceeds with unit efficiency for $H_2O^{\bullet+}$, but only 77% efficiency for $HOD^{\bullet+}$ and 67% for $D_2O^{\bullet+}$. Based on these observations, it seems likely that the reaction is kinetically controlled by an initial charge transfer, one that is subtly affected by isotope effects brought about by deuterium substitution. After this highly energetic CT reaction, there is a partitioning between separation and hydrogen (deuterium) atom transfer that does not measurably display an isotope effect.

We therefore propose the reaction mechanism shown in Figure 5. In this mechanism, all reaction channels are initiated by CT. The ion−dipole complex formed from CT, $[H_2O\ H_2C{=}CH_2^{\bullet+}]$, can then partition between separation or further reaction. As the CT is so exothermic, (49 kcal mol^{-1}, excluding ion−dipole complexation energy) there is no measurable isotope effect on the 21% of hydrogen (deuterium) atom transfer that follows. Deuterium substitution can thus impact the CT step (by a subtle change in energy-level matching) while not affecting the branching ratio. This two step mechanism is also consistent with the Rakshit and Warneck[12] observation of only CT provided their interaction energy was suprathermal. In a multistep mechanism, one expects that as the interaction energy is raised, products that correspond to an earlier portion of the mechanism should increase.[22] The simplest mechanistic picture, that of competitive CT and PT from the initial collision complex (Figure 5), seems to be inconsistent with a kinetic isotope effect on the rate of the reaction but not on the product distribution.

The reactions of HO^+ and DO^+ with $H_2C{=}CH_2$ display behavior similar to that described above for the $L_2O^{\bullet+}$ reaction. Both LO^+ reactions proceed predominantly to give formal CT product (66%). Both LO^+ reactions give a minor yield (12%) of formal hydride transfer product, producing the vinyl cation (*m*/*z* 27). The remaining 22% of the reaction products appear at *m*/*z* 29 for the HO^+ reaction. However, the DO^+ reaction reveals that this product mixture is a 2:1 mixture of formal proton (deuteron) transfer, giving $C_2H_5^+$ ($C_2H_4D^+$), and a fragmentation reaction giving HCO^+ (DCO^+).

Unlike the $L_2O^{\bullet+}$ reactions, there is neither an isotope effect on the branching ratio nor on the observed rate coefficient. Also, there are additional product channels for the LO^+ reactions. In analogy to the mechanism proposed for the $L_2O^{\bullet+}$ reaction in Figure 5, we propose a mechanism for the LO^+ reaction in Figure 6. As in the earlier case, we envision the reaction

proceeding by initial CT with the product selection occurring from the so-formed ion−molecule complex. The details of the complex fragmentation channels (leading to $C_2H_3^+$ and HCO^+) must be considered speculative at this point due to lack of detailed information (such as whether the neutrals for the $C_2H_3^+$ channels are H + OH or H_2O). The HCO^+ pathway is consistent with our observations and interpretation of the same product formed in the $O^{\bullet+}$ + $H_2C{=}CH_2$ reaction.[16] The highly exothermic nature of the CT, even more so than in the $L_2O^{\bullet+}$ + $H_2C{=}CH_2$ reaction, helps understand the greater product complexity here.

Conclusion

The 298 K ion−molecule reaction products and rate coefficients for the reaction of both $L_2O^{\bullet+}$ and LO^+ with $H_2C{=}CH_2$ are proposed to proceed initially by charge transfer. For most reactions the rate-determining step is the collision step; for reactions of $HOD^{\bullet+}$ and $D_2O^{\bullet+}$, the CT step is partially rate-determining. The product-determining steps are after the CT and, as a result, no isotope effects are found. Multiple-step mechanisms are thus proposed for both reaction series that explain all observations.

Acknowledgment. We gratefully acknowledge support of the National Science Foundation in carrying out this study.

References and Notes

(1) Smith, D. *Chem. Rev.* **1992**, *92*, 1473.
(2) Smith, D.; Spanel, P. *Mass Spectrom. Rev.* **1995**, *14*, 255.
(3) Lewis, J. S.; Prinn, R. G. *Planets and Their Atmospheres*; Academic Press: New York, 1994.
(4) Hucknall, D. J. *Chemistry of Hydrocarbon Combustion*; Chapman and Hall: London, 1985.
(5) Fialkov, A. B.; Kalinich, K. Y.; Fialkov, B. S. In: *24th Symp. (Int.) Combust.* **1992**, 785.
(6) Tanner, S. D.; Goodings, J. M.; Bohme, D. K. *Can. J. Chem.* **1981**, *59*, 1760.
(7) Harrison, A. G. *Chemical Ionization Mass Spectrometry*, 2nd ed.; CRC Press: Boca Raton, FL, 1992.
(8) Duley, W. W.; Williams, D. *Interstellar Chemistry*; Academic Press: New York, 1984.
(9) Lequeux, J.; Roueff, E. *Phys. Rep.* **1991**, *200*, 241.
(10) Lehman, T. A. *Mass Spectrom. Rev.* **1995**, *14*, 353.
(11) Dotan, I.; Lindinger, W.; Rowe, B.; Fahey, D. W.; Fehsenfeld, F. C.; Albritton, D. L. *Chem. Phys. Lett.* **1980**, *72*, 67.
(12) Rakshit, A. B.; Warneck, P. *J. Chem. Soc., Faraday Trans. 2* **1980**, *76*, 1084.
(13) Shul, R. J.; Passarella, R.; DiFazio, L. T.; Keesee, R. G.; Castleman, A. W. *J. Phys. Chem.* **1988**, *92*, 4947.
(14) Fishman, V. N.; Grabowski, J. J. *Int. J. Mass Spectrom. Ion Processes* **1998**, *177*, 175.
(15) Brink, G. O. *Rev. Sci. Instrum.* **1966**, *37*, 857.
(16) Fishman, V. N.; Graul, S. T.; Grabowski, J. J. *Int. J. Mass Spectrom. Ion Processes* **1999**, *185/186/187*, 477.
(17) Grabowski, J. J.; Melly, S. I. *Int. J. Mass Spectrom. Ion Processes* **1987**, *81*, 147.
(18) Su, T.; Chesnavich, W. J. *J. Chem. Phys.* **1982**, *76*, 5183.
(19) Anicich, V. G.; Sen, A. D. *Int. J. Mass Spectrom. Ion Processes* **1998**, *172*, 1.
(20) Ikezoe, Y.; Matsuoka, S.; Takebe, M.; Viggiano, A. *Gas-Phase Ion−Molecule Reaction Rate Constants Through 1986*; Maruzen Company, Ltd.: Tokyo, 1987.
(21) Anicich, V. G. *J. Phys. Chem. Ref. Data* **1993**, *22*, 1469.
(22) Bierbaum, V. M.; Grabowski, J. J.; DePuy, C. H. *J. Phys. Chem.* **1984**, *88*, 1389.
(23) McIntosh, B. J.; Adams, N. G.; Smith, D. *Chem. Phys. Lett.* **1988**, *148*, 142.
(24) Matthews, K. K.; Adams, N. G.; Fisher, N. D. *J. Phys. Chem. A* **1997**, *101*, 2841.